Journal of The Electrochemical Society, **155** (9) A642-A647 (2008)
0013-4651/2008/155(9)/A642/6/$23.00 © The Electrochemical Society

Phases Formed in Al-Doped $Ni_{1/3}Mn_{1/3}Co_{1/3}(OH)_2$ Prepared by Coprecipitation: Formation of Layered Double Hydroxide

Xuemei Zhao, Fu Zhou, and J. R. Dahn*,z

Department of Physics and Atmospheric Science, Dalhousie University, Halifax, Nova Scotia B3H 3J5, Canada

The coprecipitation process, using either mixed nitrate or sulfate solutions, to produce Al-doped $Ni_{1/3}Mn_{1/3}Co_{1/3}(OH)_2$ has been studied in detail. Using X-ray diffraction (XRD) and thermal gravimetric analysis (TGA), it has been determined that charge-compensating NO_3^- or SO_4^{2-} ions accompany the incorporated Al^{3+} ions into the structure to form layered double hydroxides (LDHs). The phases formed were determined for $0 < z < 1/3$ in $Ni_{1/3}Mn_{1/3}Co_{1/3-z}Al_z(OH)_2(NO_3)_z$ and $Ni_{1/3}Mn_{1/3}Co_{1/3-z}Al_z(OH)_2(SO_4)_{z/2}$. For $0 < z < 1/6$, two phase mixtures between $M(OH)_2$ (M = Ni, Mn, and Co) and the LDH phase with $z \approx 1/6$ were formed. For aluminum contents greater than $z = 1/6$, XRD and TGA experiments suggest that the excess Al is present as $Al(OH)_3$ and that the product is a mixture of $M_{5/6}Al_{1/6}(OH)_2(NO_3)_z$ or $M_{5/6}Al_{1/6}(OH)_2(SO_4)_{z/2}$ and $Al(OH)_3$, where M represents the mixture of Ni, Mn, and Co. Alternatively, the data can also be explained assuming that samples with $z > 1/6$ are single phase $Ni_{1/3}Mn_{1/3}Co_{1/3-z}Al_z(OH)_2(NO_3)_{1/6}(OH)_{z-1/6}$. TGA experiments show that the NO_3^- in the NO_3^--containing LDH is eliminated at lower temperature than the SO_4^{2-} in the SO_4^{2-}-containing LDH. Thus coprecipitations using nitrates may be preferred in situations where excellent cation mixing is desired in the production of Al-doped $Li[Ni_{1/3}Mn_{1/3}Co_{1/3-z}Al_z]O_2$.
 [DOI: 10.1149/1.2949405]

Manuscript submitted April 30, 2008; revised manuscript received June 2, 2008. Published July 15, 2008.

Layered lithium transition metal oxide compositions $Li[Ni_xCo_{1-2x}Mn_x]O_2$ have emerged as excellent new cathode materials for lithium-ion batteries.[1-9] In this series, $LiNi_{1/3}Mn_{1/3}Co_{1/3}O_2$ with $x = 1/3$ has received the most attention[2,10-13] due to its improved safety and reduced cost compared to $LiCoO_2$. The most successful synthesis method for these oxides is the mixed hydroxide method that consists of two steps.[1] The first is a coprecipitation of mixed transition metal salts in a stirred solution of LiOH or NaOH, which causes the precipitation of $M(OH)_2$ (M = Ni, Mn, and Co) with a uniform cation distribution. The second step consists of mixing the $M(OH)_2$ with a stoichiometric amount of $LiOH{\cdot}H_2O$ or Li_2CO_3 and heating the mixture in air at high temperature.

Efforts have been made to further improve the properties of $Li[Ni_xCo_{1-2x}Mn_x]O_2$ materials, including cation doping, anion doping, surface coating, etc.[14-18] Cation doping can modify the electrochemical properties of the $Li[Ni_xCo_{1-2x}Mn_x]O_2$ electrode materials. Almost all previous research has focused on the impact of cation doping on the properties of the final lithium transition metal oxide. The impact of cation doping on the intermediate mixed hydroxide product has received very little attention.

Ni, Mn, and Co hydroxides are isostructural because the transition metal cations are all divalent. The single-phase mixed hydroxide $Ni_{1/3}Mn_{1/3}Co_{1/3}(OH)_2$ phase is formed during the coprecipitation step. However, when trivalent cations like Al^{3+} are doped into the structure by the coprecipitation method, anions such as NO_3^- or SO_4^{2-}, are incorporated into the structure to compensate for the excess charge on the aluminum cation. This leads to the formation of a new phase, called a layered double hydroxide (LDH),[19-24] where anions, along with some water, are intercalated into the galleries between the $M(OH)_2$ slabs. Reference 19 gives an excellent review about the structural properties of LDH materials. Figure 1 shows the LDH structure, where a charge-compensating anion is intercalated between the HO–$M_{1-z}Al_z$–OH slabs, leading to structures like $M_{1-z}Al_z(OH)_2(NO_3)_z$, where M is a single divalent metal or a mixture of divalent metals. The intercalation of the anions leads to a large increase in the spacing between centers of the $M(OH)_2$ slabs, from about 4.60 to about 7.65 Å. In addition, the presence of the anions during the formation weakens the interactions between the slabs and leads to turbostratic misalignment (random rotations or translations parallel to the layers) and/or stacking faults between adjacent layers. In this work, the impact of Al^{3+} doping on the structure and properties of the $Ni_{1/3}Mn_{1/3}Co_{1/3-z}Al_z$ mixed hydroxide product prepared by coprecipitation is reported.

Experimental

$LiOH{\cdot}H_2O$, $Ni(NO_3)_2{\cdot}6H_2O$, $Mn(NO_3)_2{\cdot}4H_2O$, $Co(NO_3)_2{\cdot}6H_2O$, and $Al(NO_3)_3{\cdot}9H_2O$ (all from Aldrich) were used as starting materials in the preparation of NO_3^--containing LDH phases. In the case of the SO_4^{2-}-containing LDH phase, $LiOH{\cdot}H_2O$, $NiSO_4{\cdot}6H_2O$, $MnSO_4{\cdot}H_2O$, $CoSO_4{\cdot}7H_2O$, and $Al_2(SO_4)_3{\cdot}18H_2O$ (all from Aldrich) were used as starting materials. A 250 mL aqueous solution of the transition metal and Al nitrates (or sulfates) (total concentration equal to 0.4 M) and a 250 mL aqueous solution of LiOH with an appropriate concentration (enough to precipitate the metal ions) were dripped simultaneously into a stirred flask using an electronic metering pump (Masterflex C/L pump, Barnant Co.). The beakers containing the metal nitrate (or sulfate) solution or the LiOH solution and the pump tubes were washed with distilled water several times to ensure that no metal nitrates (or sulfates) or LiOH were left unreacted. The coprecipitate that appeared in the stirred flask was filtered and washed six times with distilled water to remove the residual Li salts (excess LiOH, and the formed $LiNO_3$ or Li_2SO_4). The rinsed precipitate was dried in air at 110°C overnight. A gentle grinding of 10 min in an automatic grinder (agate mortar and pestle) was used to disperse the powder before X-ray diffraction (XRD) and thermal gravimetric analysis (TGA) testing.

XRD was made using a Siemens D5000 diffractometer equipped with a copper target X-ray tube and a diffracted beam monochromator. XRD studies were made of the coprecipitate and the products

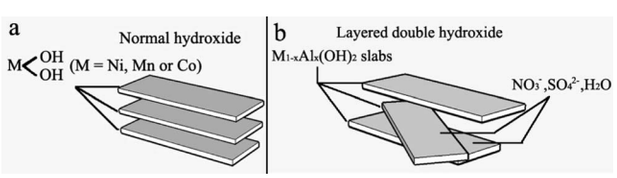

Figure 1. Schematic structures of (a) normal $M(OH)_2$ and (b) $M_{1-z}Al_z(OH)_2(NO_3)_z$ (for example) LDH. The intercalation of the anions leads to a large increase in the spacing between centers of the $M(OH)_2$ slabs, from about 4.60 to about 7.65 Å. In addition, the presence of the anions during the formation weakens the interactions between the slabs and leads to turbostratic misalignment (random rotations or translations parallel to the layers) and stacking faults between adjacent layers.

* Electrochemical Society Active Member.
z E-mail: jeff.dahn@dal.ca

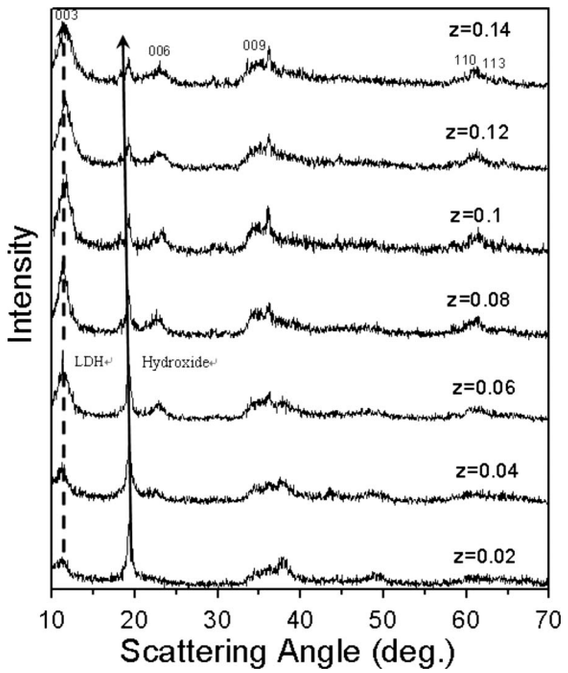

Figure 2. XRD patterns of the mixed hydroxides with different Al content, $z = 0.02$–0.14 as indicated, prepared using metal nitrate starting materials. The (001) Bragg peak of the $Ni_{1/3}Mn_{1/3}Co_{1/3}(OH)_2$ phase and the (003) Bragg peak of the $Ni_{1/3}Mn_{1/3}Co_{1/6}Al_{1/6}(OH)_2(NO_3)_{1/6}$ phase are indicated.

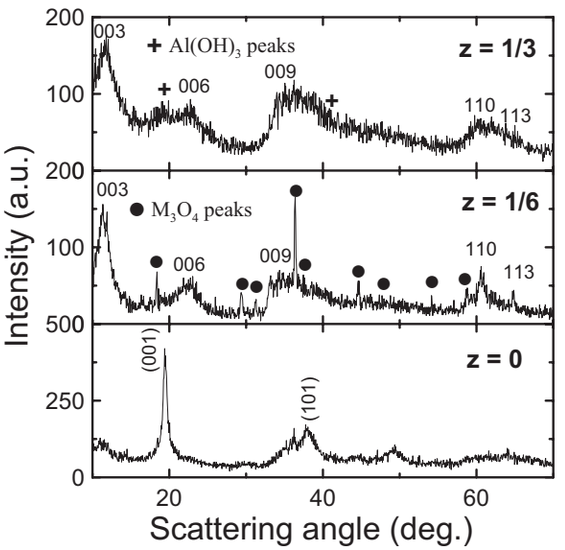

Figure 3. XRD patterns of the Ni–Mn–Co–Al mixed hydroxides with Al content, $z = 0$, 1/6, and 1/3 as indicated, prepared using metal nitrate starting materials. Some of the Miller indices of the Bragg peaks from the $Ni_{1/3}Mn_{1/3}Co_{1/3}(OH)_2$ phase and the $Ni_{1/3}Mn_{1/3}Co_{1/6}Al_{1/6}(OH)_2(NO_3)_{1/6}$ phase are indicated.

that remained after TGA. The divergence and antiscatter slits were both set to 0.5°, and the receiving slit was 0.2 mm. Data was collected in 0.05° intervals. The count time was 5 s per point.

TGA studies of the coprecipitated products were made at 5°C/min from 30 to 500 or 1000 °C in air for all the samples using a TA Instruments SDT-Q600 thermogravimetric analyzer.

Results and Discussion

Figure 2 shows typical XRD patterns of the $Ni_{1/3}Mn_{1/3}Co_{1/3-z}Al_z$ mixed hydroxides with $0.02 \leq z \leq 0.14$ after drying at 110°C in air overnight. The existence of a two-phase product is clearly observed in the XRD patterns. The solid arrow in Fig. 2 indicates the typical (001) Bragg peak of the normal $M(OH)_2$ phase, which has already been described in our earlier research.[25] Meanwhile, a new hydroxide phase is formed, as indicated by the dashed arrow, which can be ascribed to the (003) Bragg peak of the LDH phase. The Miller indices of the Bragg peaks of the LDH phase are given for the pattern for the $z = 0.14$ product, which correspond well to the typical diffraction peaks of LDH phases previously reported.[19-24] Notice the characteristic tail to higher scattering angle of the broad diffraction peak of the $z = 0.14$ sample near 35°, which indicates a large degree of turbostratic misalignment or stacking faults.

The XRD patterns in Fig. 2 show the intensity of the LDH peaks increases as z increases from $z = 0.02$ to 0.14, while the intensity of the $M(OH)_2$ peaks decreases. When the Al doping level increases to $z = 0.14$, the intensity of the $M(OH)_2$ peaks has dropped to a very low level. These results suggest that the product of coprecipitation for $0 < z <$ approx. 1/6 is a mixture of $Ni_{1/3}Mn_{1/3}Co_{1/3}(OH)_2$ and $Ni_{1/3}Mn_{1/3}Co_{1/6}Al_{1/6}(OH)_2(NO_3)_{1/6}$ phases.

Figure 3 shows the XRD patterns of the coprecipitate prepared from nitrates with Al doping levels of $z = 0$, 1/6, and 1/3. When no Al is added, no LDH is formed, as shown in the bottom of Fig. 3. As the Al content increases, the intensities of the Bragg peaks from the LDH and $M(OH)_2$ phases change accordingly, as shown in Fig. 2. The middle panel of Fig. 3 shows that when the Al content increases to $z = 1/6$, the integrated intensities of the Bragg peaks of the $M(OH)_2$ phase have dropped to a negligible level, suggesting that no $M(OH)_2$ remains in the product. Thus, when $z = 1/6$, a single LDH phase, described as $Ni_{1/3}Mn_{1/3}Co_{1/6}Al_{1/6}(OH)_2(NO_3)_{1/6}$, is obtained. There is a set of impurity peaks in the diffraction pattern for the $z = 1/6$ that arise from a hausmannite-type M_3O_4 phase. Such diffraction patterns have been observed in coprecipitated materials prepared under the deliberate introduction of oxygen.[26] Therefore, we suspect this phase appears because we did not rigorously exclude oxygen during the coprecipitation.

The top of Fig. 3 shows the diffraction pattern of the sample prepared with $z = 1/3$. This pattern appears similar to the pattern for the $z = 1/6$ sample, except for the presence of a broad diffraction peak near 18° which cannot arise from the LDH phase. We suggest that when the Al content is larger than $z = 1/6$, the extra Al cannot be accommodated into the LDH phase and is precipitated as $Al(OH)_3$. This hypothesis is examined later below, using TGA experiments. Based on the above experimental results, we suggest that the maximum Al content in the Ni–Mn–Co–Al (Al replaces Co) LDH phase is $z = 1/6$. When $z < 1/6$, the product is a two-phase system consisting of $Ni_{1/3}Mn_{1/3}Co_{1/3}(OH)_2$ and $Ni_{1/3}Mn_{1/3}Co_{1/6}Al_{1/6}(OH)_2(NO_3)_{1/6}$. When $1/6 < z \leq 1/3$, another two-phase mixture is formed after the coprecipitation synthesis, consisting of $M_{5/6}Al_{1/6}(OH)_2(NO_3)_{1/6}$ and $Al(OH)_3$.

The two-phase nature of the product for $0 < z < 0.16$ is consistent with experiments on many LDH materials reviewed in Ref. 19. In Ref. 19, Evans and Slade comment that most LDH phases cannot be prepared as single phases for $z < 0.2$, although there are some rare examples of single phases with z as low as $z = 0.07$.

TGA experiments were used in order to obtain more information about the composition of the samples. The NO_3 group has a molar mass of 62 g/mol, and the NO_3 group evolves as NO_x and oxygen along with water as the LDH phases are converted to oxide phases during heating. From the mass change during heating, the initial NO_3 content in the samples can be studied. Figure 4 shows the TGA results for samples prepared from nitrates having the following Al content: $z = 0.02$, 0.1, 1/6, 2/9, 5/18, and 1/3. The TGA curves show two typical weight loss stages. The first stage is from room temperature to around 120°C, which is assumed to be mostly due to the

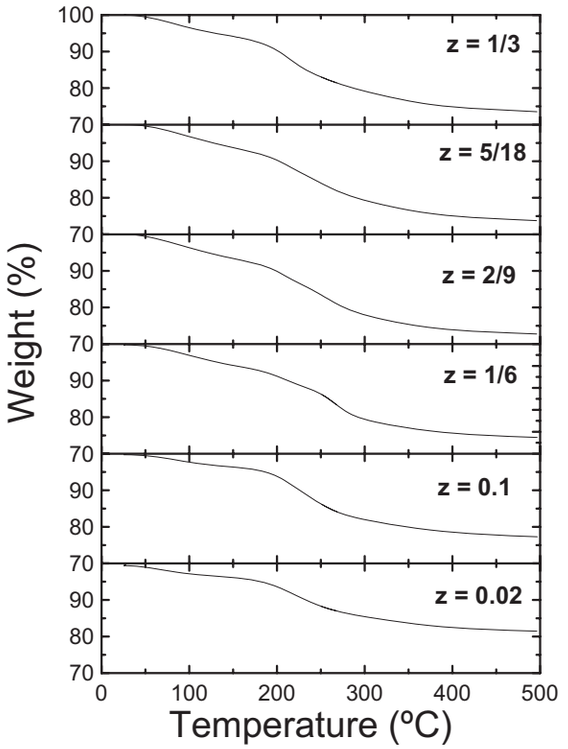

Figure 4. TGA curves of the Ni–Mn–Co–Al mixed hydroxides prepared from nitrate starting materials measured in air to 500°C. The values of the Al content, z, are indicated in each panel.

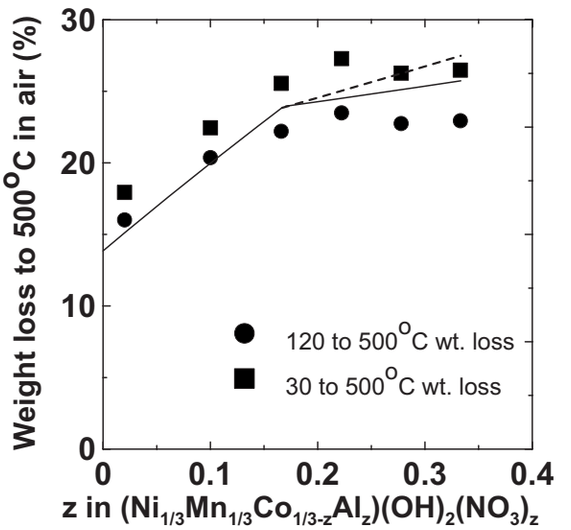

Figure 5. Comparison of the measured and calculated weight loss to 500°C of the Ni–Mn–Co–Al mixed hydroxides as a function of Al content, z. The samples were prepared from nitrate starting materials. The circles show the measured weight loss from 120 to 500°C, and the squares show the measured weight change between 30 and 500°C. The solid and dashed lines are the results of the two models described in the text.

evolution of surface or intercalated water. The second stage, taken between 120 and 500°C that contributes a large percentage to the total weight loss, is caused by the decomposition of the sample.

Our earlier work has shown that the decomposition product of $M(OH)_2$ (M = Ni, Mn, and Co) is the mixed spinel phase M_3O_4 with space group *Fd*3*m*.[25] Thus, we believe that after the TGA test in air to 500°C, the $M(OH)_2$ phase and $M_{5/6}Al_{1/6}(OH)_2(NO_3)_{1/6}$ LDH phase will transform into the M_3O_4 and $M_{2.5}Al_{0.5}O_4$ spinel phases, respectively, while $Al(OH)_3$ will decompose into Al_2O_3. Based on these assumptions, the theoretical weight loss of the samples can be calculated as a function of the Al content, z. Figure 5 shows a comparison between the calculated (solid line) and measured weight loss of the coprecipitated samples as a function of z. The square data points in Fig. 5 correspond to the measured weight loss between 30 and 500°C, while the circular data points represent the measured weight loss between 120 and 500°C. The data shows a steep upward slope in the range between $z = 0$ and 1/6. Beyond $z = 1/6$, the weight loss increases gradually with z, suggesting little, if any, further NO_3 is incorporated into the samples for $z > 1/6$. The calculated weight loss agrees well with the data and shows the needed slope change at $z = 1/6$, because we assume the excess Al, beyond $z = 1/6$, appears in the samples as $Al(OH)_3$; hence, no additional NO_3 is incorporated beyond $z = 1/6$.

Figure 6 shows the XRD patterns of samples described by Fig. 5 after the TGA test to 500°C. The diffraction patterns show very broad peaks, all of which are consistent with the expected diffraction peaks for the spinel phase. No evidence of Al_2O_3 is observed in the diffraction patterns of the samples with $z > 1/6$, but this could be amorphous. To examine this possibility, commercially available $Al(OH)_3$ (Aldrich) was heated to 500°C in the TGA and the product was shown to be amorphous by XRD as shown in Fig. 7. In addition, Wells states that the conversion of the hexagonal close-packed oxygen lattice in $Al(OH)_3$ to the cubic close-packed oxygen lattice in the spinel-type γ-Al_2O_3 requires high temperatures and long heating times.[27] Therefore, our picture of the composition of the coprecipitated samples as a function of z could be correct. One interesting result of these studies is the observation that only $Ni_{1/3}Mn_{1/3}Co_{1/6}Al_{1/6}(OH)_2(NO_3)_{1/6}$ can be prepared without the presence of other coexisting hydroxide phases. Samples with lower values of z are mixed phases with $Ni_{1/3}Mn_{1/3}Co_{1/3}(OH)_2$, and samples with higher z would be mixed phases with $Al(OH)_3$.

An alternative explanation for the results in Fig. 2-6 for $z > 1/6$ might be that beyond $z = 1/6$, the needed charge compensation for Al^{3+} is provided by intercalated OH^- ions. One reason that this might occur is that OH^- is much smaller than NO_3^-, and once the

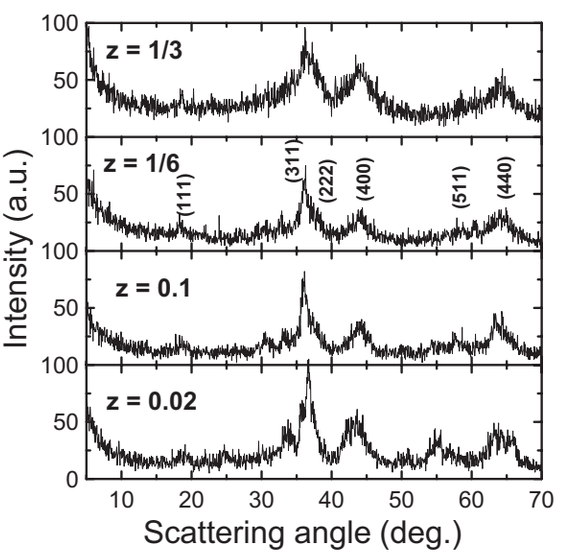

Figure 6. XRD patterns of the products of the Ni–Mn–Co–Al mixed hydroxides after TGA tests in air to 500°C. The value of the Al content, z, is indicated in each panel. The samples were prepared from nitrate starting materials.

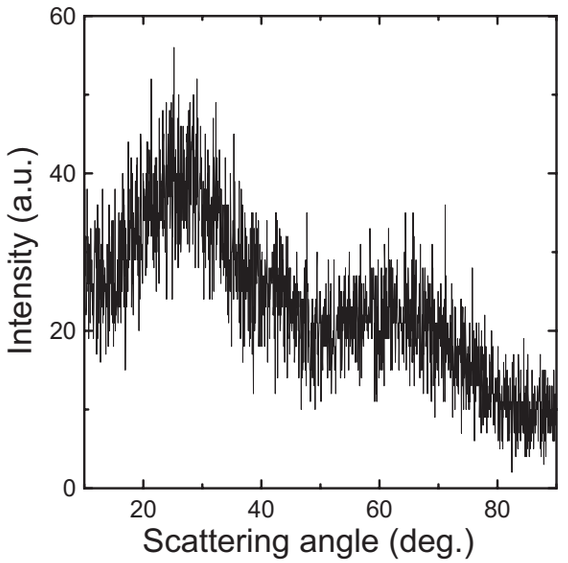

Figure 7. XRD pattern of the product of commercial $Al(OH)_3$ after a TGA test in air to 500°C.

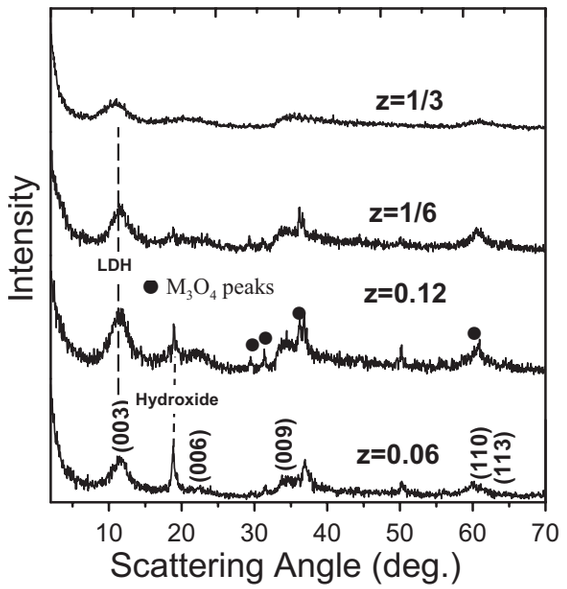

Figure 8. XRD patterns of the mixed hydroxides with different Al content, z, as indicated prepared using metal sulfate starting materials. The (001) Bragg peak of the $Ni_{1/3}Mn_{1/3}Co_{1/3}(OH)_2$ phase and the (003) Bragg peak of the $Ni_{1/3}Mn_{1/3}Co_{1/6}Al_{1/6}(OH)_2(NO_3)_{1/6}$ phase are indicated.

Al content gets high enough (at $z = 1/6$) perhaps the packing of NO_3^- ions in the galleries gets saturated. Perhaps additional OH^- could fit in spaces between the NO_3^- ions. In our experiments, the concentration of nitrate during the precipitation is almost 1 M, while the concentration of hydroxide (that which is not incorporated into the solids) is much less than 0.1 M. Thus, nitrate would be preferred as the intercalant initially, as is borne out by our experiments. To clarify if OH^- ions are intercalated into the layers after NO_3^- ions, the theoretical weight loss for this model is also calculated and shown in Fig. 5 as the dashed line. The measured weight loss data is closer to the calculated curve based on the two-phase product of $Al(OH)_3$ and $M_{5/6}Al_{1/6}(OH)_2(NO_3)_{1/6}$ than for this "dual-intercalant" model. However, further work would be required to distinguish between the $Al(OH)_3$ hypothesis or the intercalation of OH^- hypothesis to explain the reason for the change in the slope of Fig. 5 at $z = 1/6$. Such experiments are important to carry out, because according to the first hypothesis samples made with $z > 1/6$ are not single phase, while according to the second hypothesis the samples would be single phase $Ni_{1/3}Mn_{1/3}Co_{1/3-z}Al_z(OH)_2(NO_3)_{1/6}(OH)_{z-1/6}$.

Although nitrates are used in coprecipitation syntheses in research laboratories, it is more common to find sulfates used in large-scale syntheses due to their lower cost. Results on materials prepared from sulfates have been reported in the literature.[4,6,25] We performed a similar set of experiments to those described above and in Fig. 2-6 where sulfates were substituted for nitrates. In this case, because the sulfate ion is divalent, only one SO_4^{2-} for every two Al atoms is expected to be incorporated into the LDH phase.

Figure 8 shows the XRD patterns of the as-prepared mixed hydroxides with Al content, $z = 0.06$, 0.12, 1/6, and 1/3, using metal sulfates as the starting materials. Similar to the observations in Fig. 2 for the samples made with nitrates, Fig. 8 shows that for $0 < z < 1/6$, the intensity of the Bragg peaks from the LDH phase increases, while the intensity of the Bragg peaks from the $M(OH)_2$ phase decreases accordingly. The samples with $z = 0.12$ and 1/6 show some extra diffraction peaks from the M_3O_4 impurity phase, as discussed with respect to Fig. 3.

TGA measurements were also made on the samples prepared from the sulfates. Due to the high decomposition temperature of metal sulfates,[28,29] two different end temperatures were set for the TGA tests, 500 and 1000°C, respectively. Figure 9 shows the TGA results for all of the samples. The experiments which stopped at 500°C overlap perfectly with the experiments that carried on to 1000°C. The weight loss vs temperature curves show three stages. Water is evolved at low temperatures, then there is decomposition of the hydroxides to oxides between 120 and 500°C, and finally, the decomposition of whatever sulfates may have formed (during the heating to this point) around 700°C. The latter weight loss can be clearly assigned to weight loss due to sulfates by a comparison to the TGA curve of a corresponding nitrate-prepared sample.

Figure 10 compares the TGA curves for two samples with $z = 1/6$ prepared from nitrates or sulfates. The samples are believed to be pure phases of $Ni_{1/3}Mn_{1/3}Co_{1/6}Al_{1/6}(OH)_2(NO_3)_{1/6}$ and $Ni_{1/3}Mn_{1/3}Co_{1/6}Al_{1/6}(OH)_2(SO_4)_{1/12}$, respectively. Figure 10 shows

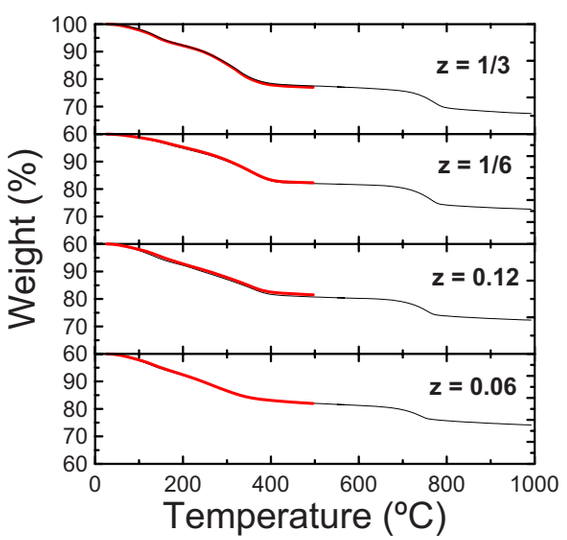

Figure 9. (Color online) TGA curves of the Ni–Mn–Co–Al mixed hydroxides prepared from sulfate starting materials measured in air to both 500 and to 1000°C. The values of the Al content, z, are indicated in each panel.

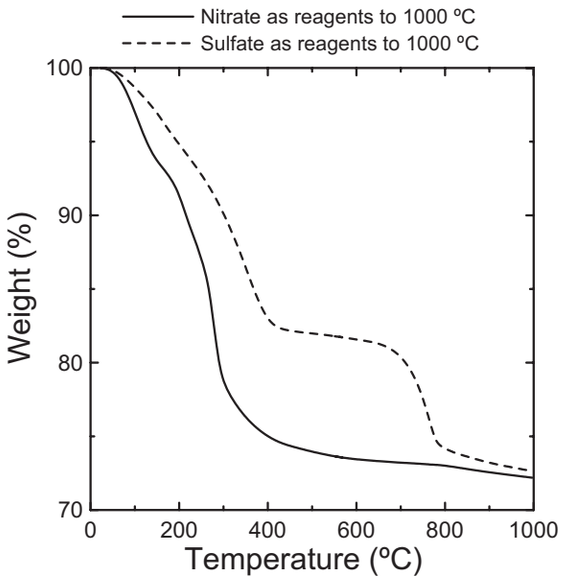

Figure 10. TGA curves of $Ni_{1/3}Mn_{1/3}Co_{1/6}Al_{1/6}(OH)_2(NO_3)_{1/6}$ (solid) and $Ni_{1/3}Mn_{1/3}Co_{1/6}Al_{1/6}(OH)_2(SO_4)_{1/12}$ (dashed) LDHs. The experiments were performed in air to 1000°C. The sharp weight loss near 700°C in the dashed curve is indicative of the loss of sulfate.

that the sample prepared from sulfates has the additional weight loss feature near 700°C which must originate from the decomposition of the sulfates.

The magnitude of the weight loss change near 700°C can be used to estimate the amount of sulfate incorporated into the samples. A cursory examination of the data in Fig. 9 shows that the magnitude of the "step" near 700°C does not scale linearly with z, especially beyond $z = 1/6$. The weight loss in the step at 700°C is almost the same for the sample with $z = 1/6$ and the sample with $z = 1/3$, suggesting that no further sulfate can be incorporated into the LDH phase beyond $z = 1/6$.

Overall, the LDH phases that form in the preparation from sulfates show a similar progression as those derived from the nitrates as the Al content, z, increases. First there is a two-phase region between $M(OH)_2$ and $M_{1-z}Al_z(OH)_2(SO_4)_{z/2}$, with $z \approx 1/6$ for $0 < z < 1/6$. For compositions with $z > 1/6$, the TGA results show that less sulfate than expected is incorporated in the structure. Again, this could be caused by formation of $Al(OH)_3$ or the formation of a single LDH phase that incorporates 1/12 SO_4^{2-} and $(z - 1/6)$ OH^-. To distinguish between these possibilities would require further work. The use of TGA coupled to a mass spectrometer would be most useful so that exhaust gases, indicating the decomposition paths, could be monitored.

Conclusions

Al-doped mixed hydroxides based on $Ni_{1/3}Mn_{1/3}Co_{1/3}(OH)_2$ were prepared by substituting Al for Co using the coprecipitation method from both nitrates and sulfates. When the Al content, $z = 0$, a pure phase of the normal hydroxide phase, $Ni_{1/3}Mn_{1/3}Co_{1/3}(OH)_2$ is prepared. When $0 < z < 1/6$, a two-phase product, consisting of the normal hydroxide $Ni_{1/3}Mn_{1/3}Co_{1/3}(OH)_2$ and the LDH $Ni_{1/3}Mn_{1/3}Co_{1/6}Al_{1/6}(OH)_2(NO_3)_{1/6}$ or $Ni_{1/3}Mn_{1/3}Co_{1/6}Al_{1/6}(OH)_2(SO_4)_{1/12}$, is produced. When $z = 1/6$, a substantially pure phase of the LDH $Ni_{1/3}Mn_{1/3}Co_{1/6}Al_{1/6}(OH)_2(NO_3)_{1/6}$ is produced. The corresponding sulfate LDH, $Ni_{1/3}Mn_{1/3}Co_{1/6}Al_{1/6}(OH)_2(SO_4)_{1/12}$, showed the presence of an M_3O_4 impurity phase but no other hydroxide phases.

In the composition range $1/6 < z \leq 1/3$, it is more difficult to determine the details of the phase or phases produced. Based on TGA experiments, it is clear that little or no further NO_3 or SO_4 is incorporated into the samples as z increases beyond $z = 1/6$. The product could be another two-phase product, composed of $M_{5/6}Al_{1/6}(OH)_2(NO_3)_{1/6}$ and $Al(OH)_3$, or a single phase with intercalated OH^- ions to compensate the charge of the additional Al^{3+} beyond $z = 1/6$. Further work is required to distinguish between these possibilities.

These results have important consequences for those involved in the production of advanced positive electrode materials for Li-ion cells. First, Al can be incorporated into a mixed hydroxide phase, but it comes along with a charge-compensating ion. Second, the Al may only be uniformly distributed in the hydroxide samples for $z = 1/6$. This is due to the two-phase nature of the product for $0 < z < 1/6$. This may have important consequences for the cation uniformity in Al-containing lithium transition metal oxides prepared from hydroxide precursors such as these. Third, the nitrate LDH phases decompose at a lower temperature than the sulfates, and this may lead to processing advantages. Finally, these Al-containing hydroxides will evolve NO_x or SO_x during their decomposition in the sintering process used to make the lithium-transition metal oxides. This may lead to the requirement for exhaust gas scrubbing equipment in industrial-scale furnaces. In order to avoid this eventuality, it is important to compare the properties of the Al-containing lithium transition metal oxides made by sintering an Al-containing mixed hydroxide, such as these, and a lithium salt with the properties of materials made from Ni–Mn–Co mixed hydroxides simply mixed with a stoichiometric amount of $Al(OH)_3$ and lithium salt followed by sintering. The latter method would lead to no toxic evolved gases but might lead to a less uniform cation distribution. Such studies are ongoing in our laboratory.

Acknowledgments

The authors acknowledge the help of Dr. Zhonghua Lu in the initial stages of this work. Funding from 3M Canada and NSERC is gratefully acknowledged.

Dalhousie University assisted in meeting the publication costs of this article.

References

1. Z. Lu, D. D. MacNeil, and J. R. Dahn, *Electrochem. Solid-State Lett.*, **4**, A200 (2001).
2. D. D. MacNeil, Z. Lu, and J. R. Dahn, *J. Electrochem. Soc.*, **149**, A1332 (2002).
3. S. Jouanneau, D. D. MacNeil, Z. Lu, S. D. Beattie, G. Murphy, and J. R. Dahn, *J. Electrochem. Soc.*, **150**, A1299 (2003).
4. S. Jouanneau, K. W. Eberman, L. J. Krause, and J. R. Dahn, *J. Electrochem. Soc.*, **150**, A1637 (2003).
5. S. Jouanneau, W. Bahmet, K. W. Eberman, L. J. Krause, and J. R. Dahn, *J. Electrochem. Soc.*, **151**, A1789 (2004).
6. J. Jiang, K. W. Eberman, L. J. Krause, and J. R. Dahn, *J. Electrochem. Soc.*, **152**, A1874 (2005).
7. C. H. Chen, C. J. Wang, and B. J. Hwang, *J. Power Sources*, **146**, 626 (2005).
8. Y. Sun, C. Ouyang, Z. Wang, X. Huang, and L. Chen, *J. Electrochem. Soc.*, **151**, A504 (2004).
9. J. K. Ngala, N. A. Chernova, M. Ma, M. Mamak, P. Y. Zavalij, and M. S. Whittingham, *J. Mater. Chem.*, **14**, 214 (2004).
10. T. Ohzuku and Y. Makimura, *Chem. Lett.*, **7**, 642 (2001).
11. N. Yabuuchi and T. Ohzuku, *J. Power Sources*, **119–121**, 171 (2003).
12. N. Yabuuchi, Y. Makimura, and T. Ohzuku, *J. Electrochem. Soc.*, **154**, A314 (2007).
13. G. Henriksen, K. Amine, J. Liu, and P. Nelson, Abstract 255, The Electrochemical Society Meeting Abstracts, Orlando, FL, Oct 12–16, 2003.
14. S. Jouanneau and J. R. Dahn, *J. Electrochem. Soc.*, **151**, A1749 (2004).
15. S. H. Na, H. S. Kim, and S. I. Moon, *Solid State Ionics*, **176**, 313 (2005).
16. M. Kageyama, D. Li, K. Kobayakawa, Y. Sato, and Y. S. Lee, *J. Power Sources*, **157**, 494 (2006).
17. H. Kim, M. Kong, K. Kim, I. Kim and H. Gu, *J. Power Sources*, **171**, 917 (2007).
18. D. Li, Y. Kato, K. Kobayakawa, H. Noguchi, and Y. Sato, *J. Power Sources*, **160**, 1342 (2006).
19. D. G. Evans and R. C. T. Slade, in *Structure and Bonding*, Series Editor, D. M. P. Mingos, Vol. 119, Layered Double Hydroxides, X. Duan and D. G. Evans, Volume Editors, pp. 1–88, Springer-Verlag, New York (2006).
20. P. Benito, F. M. Labajos, and V. Rives, *Cryst. Growth Des.*, **6**, 1961 (2006).
21. M. Kayano and M. Ogawa, *Clays Clay Miner.*, **54**, 382 (2006).
22. Y. Wang, W. Yang, S. Zhang, D. G. Evans, and X. Duan, *J. Electrochem. Soc.*, **152**, A2130 (2005).

23. J. C. Villegas, O. H. Giraldo, K. Laubernds, and S. L. Suib, *Inorg. Chem.*, **42**, 5621 (2003).
24. D. Shan, S. Cosnier, and C. Mousty, *Anal. Chem.*, **75**, 3872 (2003).
25. S. Jouanneau and J. R. Dahn, *Chem. Mater.*, **15**, 495 (2003).
26. K. Lee, S. Myung, H. J. Bang, S. Chung, and Y. Sun, *Electrochim. Acta*, **52**, 5201 (2007).
27. A. F. Wells, *Structural Inorganic Chemistry*, 5th ed., Oxford University Press, New York (1984).
28. N. G. Apte, E. Kiran, and J. V. Chernosky, *J. Therm. Anal.*, **34**, 975 (1988).
29. M. Olszak-Humienik and J. Mozejko, *Thermochim. Acta*, **344**, 73 (2000).